



# Nanoporous AISBA-15 catalysed Claisen–Schmidt condensation for the synthesis of novel and biologically active chalcones

Palani Elamathi<sup>2</sup> · Govindasamy Chandrasekar<sup>1</sup> · M.M. Balamurali<sup>2</sup>

Published online: 20 January 2020  
© Springer Science+Business Media, LLC, part of Springer Nature 2020

## Abstract

Mesoporous AISBA-15 catalysts ( $n_{Si}/n_{Al}$  ratios of 41, 129 and 210) were synthesized by sol–gel method. These materials were characterized by XRD,  $N_2$  sorption, FTIR, TPD- $NH_3$ , FESEM, EDX, and TEM analysis. XRD analysis of AISBA-15 catalysts confirmed the existence of well-ordered crystalline structure having  $p6mm$  symmetry.  $N_2$  sorption isotherm of AISBA-15 catalysts showed a type IV adsorption isotherm with H1 hysteresis loops. SEM analysis of AISBA-15 (41) indicated worm-like particle morphology with a size range of 3  $\mu m$  with co-occurrence of smaller particles of size ca. 1  $\mu m$ . TEM analysis of AISBA-15 (41) showed existence of uniform array of tubular nano-channels. The catalytic application of AISBA-15 catalysts was tested on industrially important chalcones synthesis via Claisen–Schmidt condensation reaction in environment friendly approach. The reaction parameters such as time, temperature,  $n_{Si}/n_{Al}$  ratio, catalyst amount, and catalyst stability were investigated. AISBA-15 (41) catalyst showed an excellent catalytic performance with 98% 1-tetralone conversion with 100% selectivity of compound 1c (91% yield) within 120 min AISBA-15 (129) and AISBA-15 (210) catalysts. The anti-oxidant activity of the synthesised chalcones were investigated by various in-vitro procedures, including radical scavenging potentials-1, 1-diphenyl-2-picryl-hydrazil, hydrogen peroxide scavenging, and ferric reducing potential assay. The new chalcone derivatives synthesised in this work showed a very good antioxidant activity and some were found to be more active than the parent chalcones, (E)-3-(4-hydroxy-3-methoxyphenyl)-1-phenylprop-2-en-1-one (compound 8c), and standard antioxidant (curcumin).

**Keywords** AISBA-15 · Claisen–Schmidt condensation · Chalcones · Antioxidant · HSA binding

## 1 Introduction

Chalcones ( $\alpha$ ,  $\beta$ -unsaturated ketones) are being attracted owing to their potential applications in chemical and bio-sciences as they are used as chemical intermediates, antioxidants, biomolecular carriers and possess high drug efficacy

[1–11]. Generally, chalcones are catalysed by both acid and base catalysts such as alkaline hydroxides, sodium ethoxides [12, 13], HCl [14],  $AlCl_3$  [15], and  $BF_3$  [16]. Since these catalysts are in homogeneous nature, they remain in the reaction mixture and produce huge amounts of hazardous chemical wastes. Hence there is a huge demand in the field of catalysis to change the conventional homogenous catalysts to heterogeneous nature for them to be environment friendly and reusable following an economical route for large-scale industrial production of fine chemical synthesis.

Mesoporous AISBA-15 is considered as an excellent candidate to be used as heterogeneous solid acid catalyst owing to its exceptional textural properties of large surface area ( $\sim 700$   $m^2/g$ ), narrow distribution of pore size from 4.5 to 30 nm and a pore wall thickness between 3 and 6 nm, accompanied with high thermal and hydrothermal stability (upto  $\sim 800$   $^\circ C$ ) and strong Brønsted and Lewis acidity [17–19]. Thus, herein we introduce mesoporous AISBA-15 catalysts for the eco-friendly synthesis of vanillin derived

**Electronic supplementary material** The online version of this article (<https://doi.org/10.1007/s10934-019-00854-3>) contains supplementary material, which is available to authorized users.

✉ Govindasamy Chandrasekar  
gc\_sekar78@yahoo.co.in; carevathy@iau.edu.sa

✉ M.M. Balamurali  
mmbala@gmail.com

<sup>1</sup> Basic and Applied Scientific Research Center, College of Science, Imam Abdulrahman Bin Faisal University, P.O. Box 31441, Dammam, Saudi Arabia

<sup>2</sup> Chemistry Division, School of Advanced Sciences, Vellore Institute of Technology, Chennai, India

new chalcones (Scheme 1 I [8c]) with their structure similar to naturally available curcumin (Scheme 1 II) [2, 3].

Further, we have investigated the biological applications of these chalcones to get insights on their pharmacological properties and towards designing new therapeutic agents [20–27]. It is well known that free radicals, being produced as unavoidable products of many biochemical reactions, have both beneficial and destructive characteristics [7, 28, 29] and they play an significant role in the pathogenesis of several oxidative stress related diseases [30]. Presently available synthetic antioxidants in the market are suspected to cause liver damage and act as carcinogens. Therefore search for new antioxidant drugs of natural origin [8, 10, 31, 32] with fewer side effects is desirable and is a very active domain in medical research.

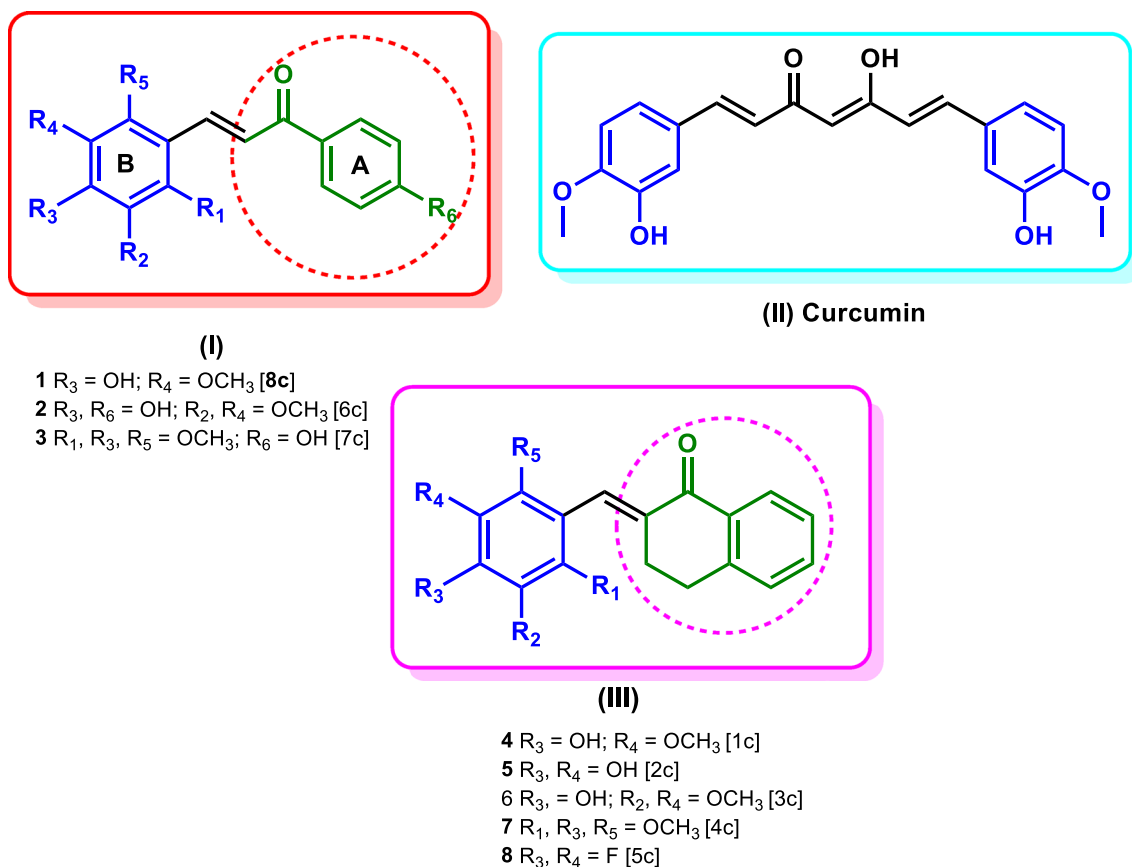
For the first time in literature, we report an efficient catalytic system for the synthesis of novel vanillin derived chalcone and its derivatives via Claisen–Schmidt condensation reaction between 1-tetralone and vanillin derivatives catalyzed by environmentally friendly heterogeneous mesoporous AISBA-15 solid acid catalysts (Scheme 2). The efficiency of AISBA-15 catalysts was studied on the

synthesis of chalcones by monitoring various reaction parameters such as time, temperature,  $n_{S1}/n_{A1}$  ratio in the catalysts, and catalyst amount. The potential applications of synthesised new chalcone derivatives were tested for their antioxidant potentials and protein binding ability. The new chalcones reported herein exhibit excellent biological properties and their biological activities were comparable to that of the natural product curcumin.

## 2 Experimental

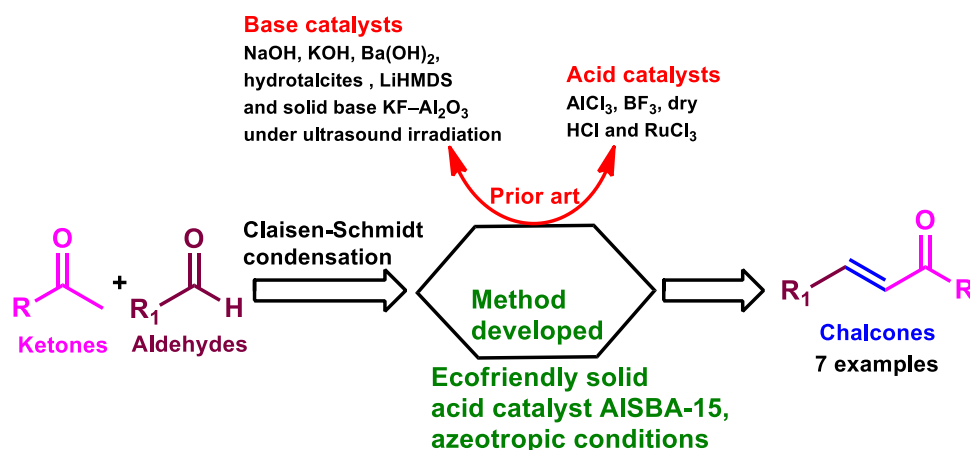
### 2.1 Materials

Tetraethyl orthosilicate (TEOS), aluminium isopropoxide, nonionic triblock copolymer (P123) was purchased from Sigma-Aldrich. Aldehydes, tetralone and acetophenone, DPPH, phenanthroline, ferrous sulphate, and potassium ferricyanide and other reagents were purchased from Rankem and SRL chemicals and were used without further purification.



**Scheme 1** (I) Acetophenone with vanillin derived chalcone and its derivatives, (II) curcumin, and (III) tetralone with vanillin derived chalcone and its derivatives

**Scheme 2** Synthesis of new chalcone and its derivatives using AISBA-15 solid acid catalyst



## 2.2 Instrumentation

A powder X-ray diffractometer (Smart lab, Rigaku, Japan) was used to get the structural patterns of AISBA-15 catalysts. With the help of Quantachrome Autosorb 1 sorption analyzer, USA, the Nitrogen sorption isotherms were obtained. Scanning electron microscopy (SEM) and energy dispersive X-ray spectroscopy (EDX) analysis was performed using a Hitachi S-4800 instrument. Transmission electron microscopy (TEM) analysis was investigated using a Hitachi H-7560 electron microscope. FT-IR measurements were performed on scientific-NICOLET IS10 (USA). The temperature-programmed desorption (TPD) of pyridine was performed on different AISBA-15 materials by using high resolution thermogravimetric analyser (SETARAM setsys 16MS) at a heating rate of 10 °C/min from 120 to 600 °C under N<sub>2</sub> flow (50 ml/min). Thin layer chromatography (TLC) was carried out using Merck 60 F254 pre-coated silica gel plate (0.2 mm thickness). Gas chromatography was used for the quantitative analysis (Thermo Scientific TRACE1300, USA) equipped with DB-5 capillary column (30 m, 0.32 mm and a film thickness of 1 micron), flame ionization detector with nitrogen carrier gas and using *n*-decane as an internal standard. BRUKER AVANCE III, 400 MHz spectrometer was used to collect the <sup>1</sup>H NMR, <sup>13</sup>C NMR spectra using tetramethylsilane as internal standard.

## 2.3 Catalyst synthesis procedure

The mesoporous AISBA-15 catalysts were synthesised by following the optimised procedure with a molar gel composition of TEOS: 0.03–0.14 Al<sub>2</sub>O<sub>3</sub>: 0.016 P123: 0.96 HCl: 126 H<sub>2</sub>O [17]. The typical synthesis procedure involves the addition of triblock copolymer of P123 to water and HCl in the stirring condition to obtain a clear solution. To this solution

required quantity of TEOS and aluminium isopropoxide were added and stirred continuously for 24 h at 40 °C. The resultant gel was aged for 48 h at 100 °C, and then the products thus obtained were filtered, dried and calcined at 550 °C for 6 h. The AISBA-15 materials were labeled as AISBA-15 (*x*), *x* where represents *n*<sub>Si</sub>/*n*<sub>Al</sub> ratio in the synthesis gel.

## 2.4 General method of chalcone synthesis

The catalytic activity of AISBA-15 (*x*) acid catalysts was tested with Claisen–Schmidt condensation reaction. Under azeotropic conditions the condensation reaction was carried out in toluene medium using Dean–Stark apparatus, with 1:1 mol ratio of aryl aldehydes and 1-tetralone in presence of AISBA-15 (41) catalyst. The kinetics of the reaction was monitored quantitatively by using gas chromatography. Samples for analysis were prepared in ethyl acetate and filtered with the help of a nylon syringe filter. Catalyst was filtered off from the reaction mixture and successively washed with toluene, hexane and ethyl acetate. The isolation of product was done by solvent evaporation and followed by recrystallization from absolute ethanol.

The catalytic activity was evaluated by monitoring the percentages of conversion of reactants, selectivity of products formed, and the yield of products isolated under selected conditions. A calibration graph was plotted from which relative response factor (RF) of the reactants and products were calculated. The below equations were followed to obtain:

$$\%Conversion = \frac{Initial\ mmoles_{reactant} - Final\ mmoles_{reactant}}{Initial\ mmoles_{reactant}} \times 100$$

$$\%Selectivity = \frac{mmoles_{product1}}{mmoles_{product1} + mmoles_{product2}} \times 100$$

$$\% \text{Isolated yield} = \frac{\text{Isolated yield(g)product}}{\left( \frac{\text{Amount of reactant (g)}}{\text{Molecular weight of reactant}} \times \text{Molecular weight of product} \right)} \times 100$$

The confirmation of the products was monitored with their melting point,  $^1\text{H}$  NMR,  $^{13}\text{C}$  NMR and FTIR spectroscopy. The results are showed in Table 3.

## 2.5 Antioxidant activity studies

The antioxidant performance of the synthesized chalcones were investigated by following their ability to scavenge radicals like DPPH, hydroxyl and by their reducing potential. The procedure adopted for each were reported elsewhere [7, 28, 29] with little modifications.

### 2.5.1 DPPH radical scavenging assay

The reaction was carried in a mixture containing 0.05 M acetate buffer, pH 5.5 and 100  $\mu\text{M}$  ethanolic solution of DPPH. To this solution, varying concentrations of the samples were added and incubated at 25  $^\circ\text{C}$  for 30 min. The scavenging ability was obtained from the change in optical density at 517 nm.

### 2.5.2 Hydrogen peroxide scavenging assay

Different concentrations of samples in the range from 0 to 200  $\mu\text{M}$  was added to a reaction mixture of 100 mM phosphate buffer, pH 5.5, 750  $\mu\text{M}$  each of ethanolic solution of phenanthroline and ferrous sulphate and 10% hydrogen peroxide. The reaction mixture was kept at 37  $^\circ\text{C}$  for 60 min. The scavenging ability was calculated by monitoring the change in optical density at 536 nm.

### 2.5.3 Reducing potential assay

The reducing potential was calculated in a reaction mix containing 100 mM phosphate buffer, pH 6.8 and 0.5% potassium ferricyanide. Varying concentrations ranging from 0 to 200  $\mu\text{M}$  of test samples in methanol was added and kept in a water bath at 50  $^\circ\text{C}$  for 20 min. The reaction was quenched by adding 3% (w/v) trichloroacetic acid followed by centrifugation at 10,000 $\times g$  or RFC (Relative Centrifuge Force) for 10 min at room temperature using a centrifuge (model: Remi CPR24 plus) with a rotor (model: R-248 M) radius of 84 mm. Since the rpm is not uniform for centrifuges with different rotor radius, we maintained RCF instead of rpm for the uniform centrifugal operations. However, for the value of 10,000 $\times g$ , the corresponding rpm calculated was 10,310 using the formula  $\text{RCF} = 1.12 \times \text{rotor radius} \times (\text{rpm}/1000)^2$ . To the above supernatant,  $\sim 0.01\%$  of ferric chloride was

added and the change in absorbance value was monitored at 700 nm using UV–Visible spectrophotometer.

In all the above, the blank reaction was performed without the test samples. The scavenging abilities are reported either as  $\text{EC}_{50}$  or as % scavenging.

## 2.6 HSA binding studies

### 2.6.1 Fluorescence quenching studies

The ability of the synthesised chalcones to interact with human serum albumin was analysed by fluorescence titration method. The interaction studies were performed by titrating various concentrations of the sample against 5  $\mu\text{M}$  HSA in 10 mM phosphate buffer, pH 7.4. After each addition of test sample, the fluorescence emission scan was done between 310 to 550 nm by exciting at 295 nm. The quenching of fluorescence was monitored by following Stern–Volmer equation (Eq. 1). The results are depicted in Table 5. The Scatchard equation (Eq. 2) was employed to evaluate the binding constant and number of binding sites.

$$\frac{F_0}{F} = 1 + K_{SV}[Q] = 1 + K_q\tau_0[Q] \quad (1)$$

where,  $F$  and  $F_0$  are relative fluorescence responses of HSA in presence and absence of quencher, i.e. chalcones, respectively,  $[Q]$  is total concentration of quencher,  $\tau_0$  is average fluorescence lifetime of fluorophore alone ( $\tau_0 = 10^{-8}$  s) without the presence of quencher and  $k_q$  is apparent value of bimolecular quenching constant, which is obtained from the ratio of  $K_{SV}:\tau_0$ . The slope of linear graph obtained by plotting  $F_0/F$  against  $[Q]$  for each sample gives the value of  $K_{SV}$ . The binding constant ( $K_b$ ) and the number of binding sites ( $n$ ) on HSA are obtained from linear plot of  $\log(F_0 - F/F)$  versus  $\log [Q]$  following Eq. 2.

$$\log\left(\frac{F_0 - F}{F}\right) = \log K_b + n \log [Q] \quad (2)$$

## 3 Results and discussion

### 3.1 Catalyst characterization

The structural properties of AISBA-15 were investigated by X-ray diffraction patterns. As seen in Fig. 1, the XRD pattern of the catalysts showed an intense peak at  $2\theta$  value

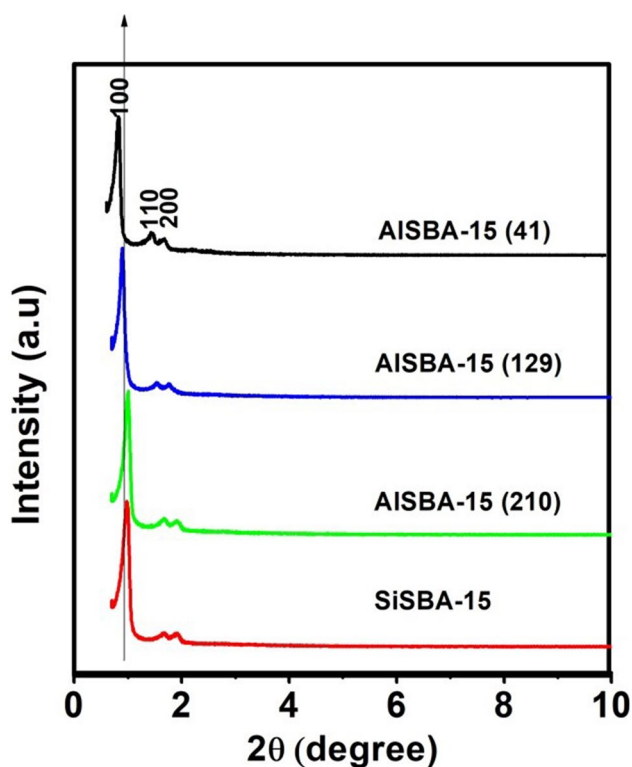


**Fig. 1** The XRD patterns of AISBA-15 with different  $n_{\text{Si}}/n_{\text{Al}}$  ratio (a) low angle, and (b) high angle

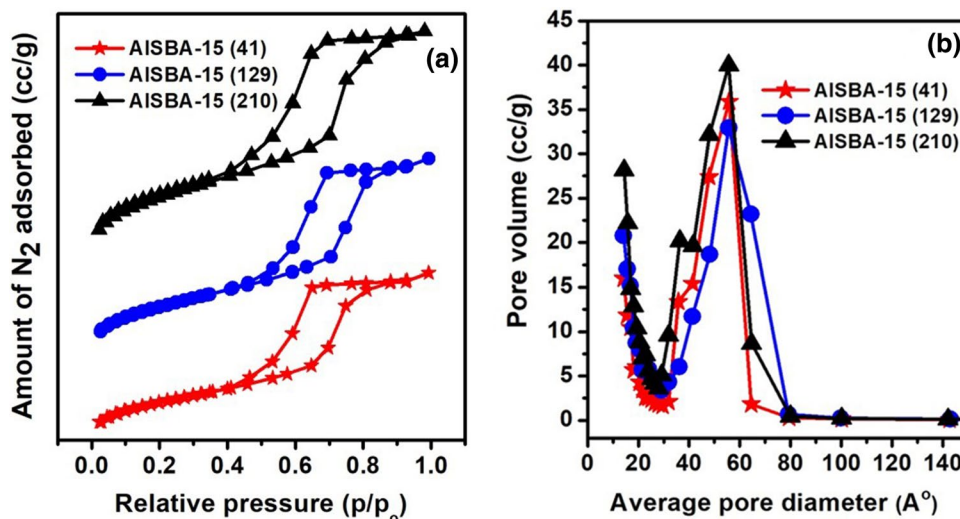
of 0.87 followed by two weak peaks at 0.93 and 0.96 that respectively correspond to (100), (110) and (200) reflections. The results clearly indicate the presence of  $p6mm$  hexagonal symmetry in all the AISBA-15 catalyst materials. As the Al content increased in synthesis gel due to the replacement of  $\text{Al}^{3+}$  (ionic radii 0.57 Å) by  $\text{Si}^{4+}$  (ionic radii of 0.26 Å) in silica framework (Table 1), the lattice parameters

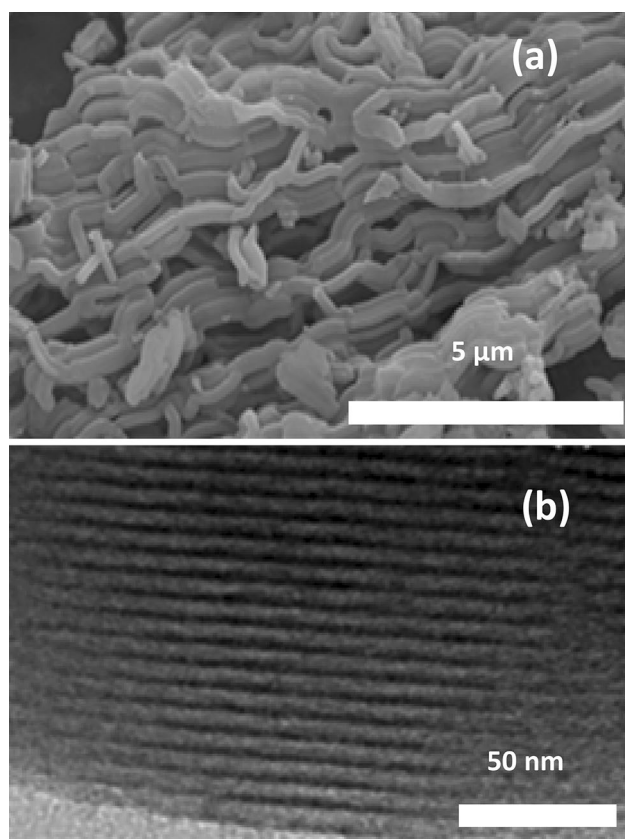
including the  $d$  spacing and  $a_o$  of AISBA-15 catalysts also have increased considerably. A broad peak at  $2\theta = 24$  due to amorphous silica and absence of any peak due to aluminium oxide in AISBA-15 samples is observed in the high angle XRD patterns (Figure S1) of AISBA-15 catalysts indicate the absence agglomerated aluminium oxide [33].

Figure 2 depicts the  $\text{N}_2$  sorption isotherms (a) and BJH pore size distribution (b) of AISBA-15. The catalysts showed type IV isotherms with  $\text{H}_1$  hysteresis loop. The textural properties of AISBA-15 catalysts are given in Table 1. As the aluminium content in catalyst decreases, it is observed that the surface area and the pore volume increase respectively from 480 to 757  $\text{m}^2 \text{g}^{-1}$  and 0.6 to 0.93  $\text{cm}^3 \text{g}^{-1}$ . This is due to the increase of Al contentment in the mesoporous AISBA-15 may leads to the formation of minor quantity of  $\text{Al}_2\text{O}_3$  oxide in the mesopores, can decrease pore volume and surface area. Further, the increase in pore size is due to the replacement of  $\text{Al}^{3+}$  ions (ionic radii 0.57 Å) by  $\text{Si}^{4+}$  (ionic radii of 0.26 Å) ions in silica framework. This was further evidenced from XRD measurements is that as Al content increases, the lattice parameters (including the  $d$  spacing and  $a_o$ ) of AISBA-15 catalysts increases considerably. A narrow range BJH pore size distribution is observed with an average pore diameter of ca. 55 Å is observed for AISBA-15 [17].

Table 1 presents the data obtained from pyridine adsorbed temperature programmed desorption (TPD) of all samples. The samples of AISBA-15, exhibits pattern of three different weight losses; which correspond to sites with weak (weight loss between 120 and 350 °C), moderate (351 and 450 °C), and strong (451 and 600 °C) acidic characters. The surface hydroxyl groups could be responsible for weak acid sites, while medium and strong acid sites could have initiated from aluminium incorporated into the framework of silica. The number of weak acid sites increases as  $n_{\text{Si}}/n_{\text{Al}}$  ratio increases. This could be ascribed to increase in weakly

**Fig. 2** The nitrogen sorption isotherms (a) and BJH pore size distribution (b) of AISBA-15 catalysts





**Fig. 3** a SEM, b TEM image of AISBA-15 (41) catalyst

attached hydrogen bonded pyridine molecules on the terminal silanol groups. However, number of medium and strong acid sites decreases with increase in ratio of  $n_{\text{Si}}/n_{\text{Al}}$ .

The (a) SEM and (b) TEM image of AISBA-15 (41) are depicted in Fig. 3. The SEM image displayed particles with a worm like structure of ca. 3  $\mu\text{m}$  with co-existence of smaller particles of ca. 1  $\mu\text{m}$ . The elemental compositions of AISBA-15 catalyst samples observed from EDX analysis are shown in Table 1. It was observed that  $n_{\text{Si}}/n_{\text{Al}}$  ratio of calcined AISBA-15 catalysts is higher than that of  $n_{\text{Si}}/n_{\text{Al}}$  ratio in the synthesis gel. This could be due to high solubility of aluminium isopropoxide in acidic medium. The TEM image of AISBA-15 (41) catalyst indicated the presence of a well-ordered close packed array of one-dimensional mesoporous channels.

The vibrational spectra of AISBA-15 samples are depicted in Fig. 4. Prominent bands were observed at 1088, 803, 956, 1376, and 3400–3500  $\text{cm}^{-1}$ . The anti-symmetric and symmetric stretching vibration bands of Si–O–Si are observed at 1088  $\text{cm}^{-1}$  and 803  $\text{cm}^{-1}$  respectively, to while the anti-symmetric of Si–O–Al appears at 956  $\text{cm}^{-1}$ . A broad band in the range of 3400–3500  $\text{cm}^{-1}$  could be assigned to framework surface Si–OH groups. The band at 1376  $\text{cm}^{-1}$  is due to the adsorbed water molecules on AISBA-15 samples [33].

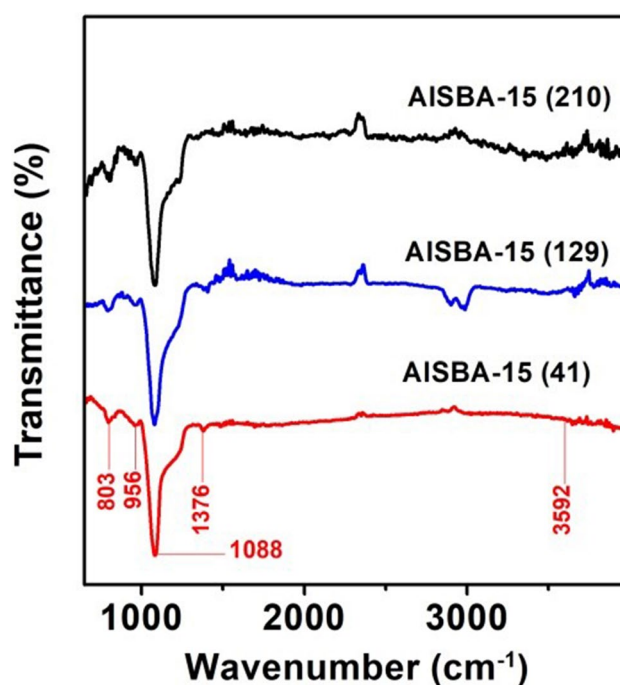


**Fig. 4** FT-IR spectra of AISBA-15 catalysts with different  $n_{\text{Si}}/n_{\text{Al}}$  ratio

## 3.2 Catalytic activity

The catalytic investigation on the synthesis of chalcones was successfully tested using AISBA-15 solid acid catalysts with different aldehydes and 1-tetralone using azeotropic reaction method. The influence of AISBA-15 catalysts were analysed on different reaction parameters including time, temperature,  $n_{\text{Si}}/n_{\text{Al}}$  ratio of AISBA-15, catalyst amount, solvent and catalyst stability to synthesis (E)-2-(4-hydroxy-3-methoxybenzylidene)-3,4-dihydronaphthalen-1(2H)-one (Compound 1c).

### 3.2.1 Effect of reaction time

The catalytic performance of (conversion of 1-tetralone and selectivity to compound 1c) of AISBA-15 (41) catalyst was tested in a catalytic reaction, carried out at 100  $^{\circ}\text{C}$  using 100 mg catalyst under azeotropic condition on different reaction time viz., 10, 15, 30, 60, 90, 120, 150, and 180 min is indicated in Fig. 5. It was inferred that the conversion of 1-tetralone is gradually increased from 52.4 to 100% upon increasing the reaction time from 10 to 180 min. As the reaction time increases from 10 to 120 min, the selectivity of compound 1c remains constant at about 100%, beyond which it falls down to 88%, when the reaction time is increased to 180 min. The decrease

**Table 1** Elemental composition and textural properties of AISBA-15 catalytic materials

$n_{Si}/n_{Al}$ (gel)	$n_{Si}/n_{Al}$ (product)	$a_0$ (Å)	$d_{100}$ (Å)	$S_{BET}$ (m <sup>2</sup> /g)	$D_p$ (Å)	$V_p$ (m <sup>3</sup> /g)	Total acidic sites (mmol/g)
7	41	116	101	480	54	0.65	0.42
14	129	109	94	563	53	0.76	0.20
28	210	102	91	757	49	0.93	0.11

$S_{BET}$  specific surface area,  $V_p$  pore volume,  $D_p$  pore diameter,  $a_0$  unit cell constant was calculated as,  $a_0 = 2 \times d_{100} / \sqrt{3}$

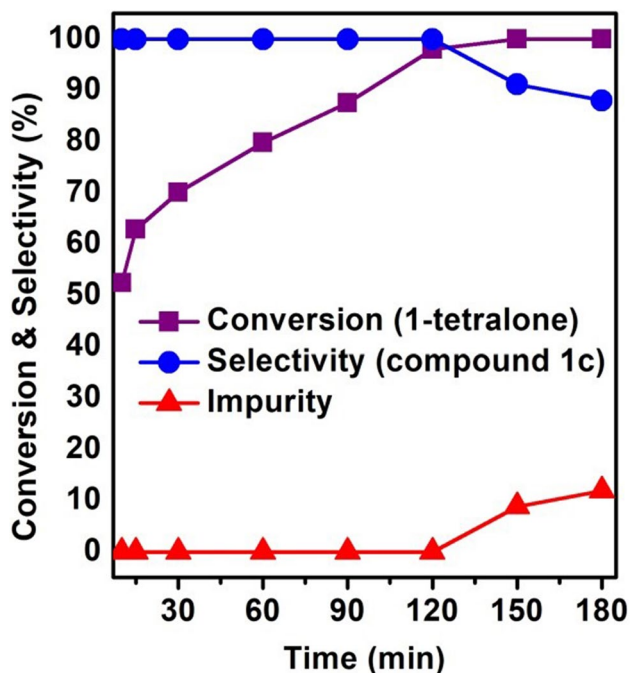


**Fig. 5** Effect of reaction time in the synthesis of compound 1c. Vanillin (0.0034 mol), 1-tetralone (0.0034 mol), AISBA-15 (41) (100 mg), toluene (10 ml) under azeotropic conditions

in selectivity of compound 1c at longer reaction time is due to the formation of coke on catalytic active sites by strong adsorption of reactants and/or products, and favours formation of impurities [34]. From this study the optimum reaction time was fixed as 120 min to get maximum 1-tetralone conversion of 98% and selectivity of 100% for compound 1c.

### 3.2.2 Effect of $n_{Si}/n_{Al}$ ratio

The catalytic reaction for the synthesis of compound 1c was carried out using AISBA-15 catalysts ( $n_{Si}/n_{Al}$  ratios of 41, 129 and 210) with the following reaction conditions: 100 mg of catalyst, 100 °C (azeotropic conditions), and 120 min and the results are presented in Fig. 6. The isolated yield of compound 1c decreased from 91 to 64% as  $n_{Si}/n_{Al}$  ratio increased from 129 to 210. This clearly infers as the

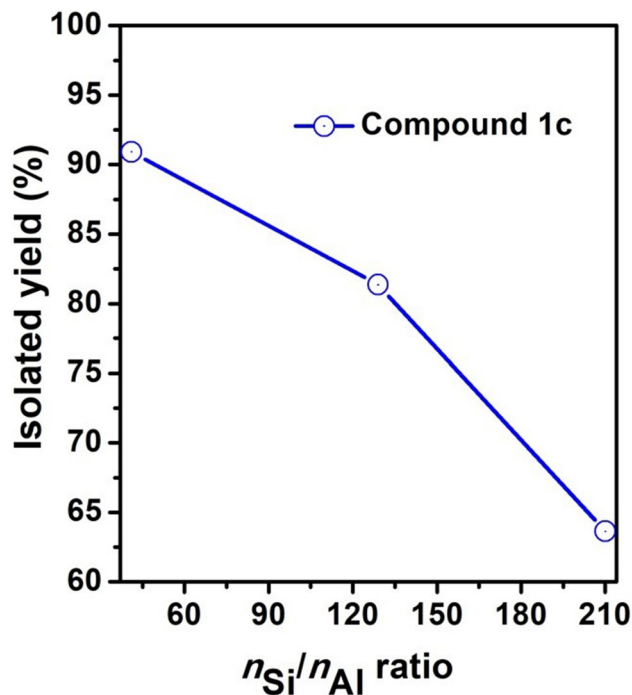


**Fig. 6** Effect of  $n_{Si}/n_{Al}$  ratio of AISBA-15 catalysts in the synthesis of compound 1c. Vanillin (0.0034 mol), 1-tetralone (0.0034 mol), AISBA-15 (100 mg), toluene (10 ml), 120 min under azeotropic conditions

number of acidic sites decrease in the catalytic materials, the product yield is decreases. It indicates us the product yield is mainly governed by the number of acidic sites present on the catalytic materials and the number of acidic sites is comparatively higher in AISBA-15 (41) than in AISBA-15 (129) and AISBA-15 (210). These acidic sites catalyse the reactants more effectively to give excellent yields up to 91% (Table 1). Moreover, AISBA-15 (41) has a pore size of 54 Å which is 1.9% and 9.3% larger than that in AISBA-15 (129) and AISBA-15 (210), respectively. The AISBA-15 (41) with large pore size of 54 Å facilitates the faster diffusion of reactants into the nano-channels with minimum constrain to get adsorbed on the active sites and transform to product that can easily diffused out [35]. This could also add to the reason for high product yield (91%) of compound 1c

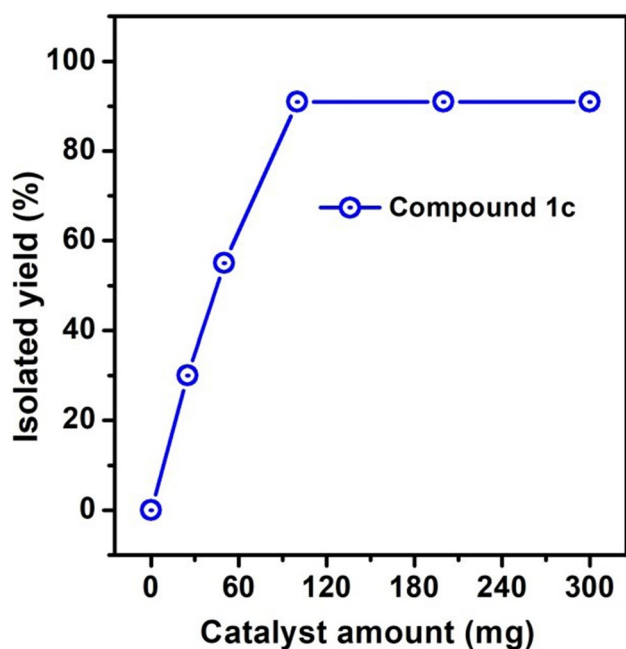


**Fig. 7** Effect of AISBA-15 (41) catalyst amount in the synthesis of compound 1c. Vanillin (0.0034 mol), 1-tetralone (0.0034 mol), toluene (10 ml) under azeotropic conditions

within 120 min using AISBA-15 (41) catalyst as compared to AISBA-15 (129) and AISBA-15 (210).

### 3.2.3 Effect of catalyst amount

The study on the effect of catalyst amount for compound 1c synthesis was carried out with different amount of AISBA-15 (41) catalyst ranging from 0 to 300 mg and product yield is depicted in Fig. 7. The reaction was carried out in an azeotropic mixture of vanillin and 1-tetralone with 1:1 ratio at 100 °C for 120 min in the presence and absence of AISBA-15 (41) catalyst. The reaction did not proceed towards product in the absence of catalyst. But when 25 mg of AISBA-15 (41) catalyst was added, 30% yield of compound 1c was observed. This indicates the significant presence of acidic sites in AISBA-15 (41) catalyst to catalyse the Claisen–Schmidt condensation reaction. Increase of catalyst amount from 25 to 100 mg in the reaction, increased the yield of compound 1c to 61%. This could be due to the eventual increase in active sites contributed from the catalyst in reaction medium to catalyse the reaction. Upon further increase of catalyst amount from 200 to 300 mg, no intensification of the product formation was observed, as the number of reactants is less compared to the active sites of the excess catalysts in the reaction mixture. Therefore, it is evident from this study that 100 mg of AISBA-15 (41) acid catalyst would be an ideal quantity to convert vanillin and 1-tetralone to compound 1c to yield product up to 91%.

**Table 2** AISBA-15 (41) catalysed Claisen–Schmidt condensation at different reaction temperature

Entry	Reaction temperature (°C)	Yield (%) <sup>a</sup>
1	RT	0
2	40	0
3	60	25
4	90	75
5	100	84
6	110	85
7 <sup>b</sup>	<b>100</b>	<b>91</b>
8 <sup>b</sup>	110	86

Reaction conditions: Vanillin (0.0034 mol), 1-tetralone (0.0034 mol), AISBA-15 (41) (100 mg), toluene (10 ml), reaction time 120 min

The results with optimized reaction temperature are shown in bold

<sup>a</sup>Isolated yield

<sup>b</sup>Azeotropic method

### 3.2.4 Effect of reaction temperature

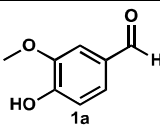
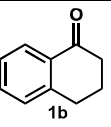
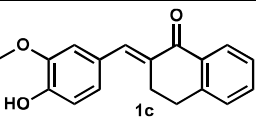
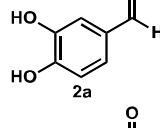
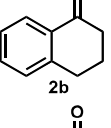
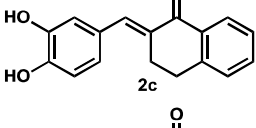
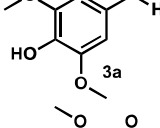
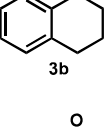
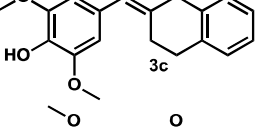
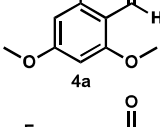
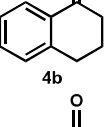
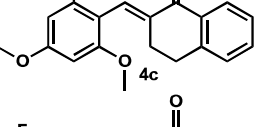
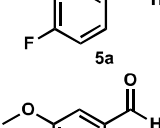
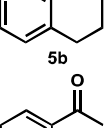
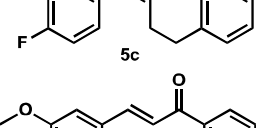
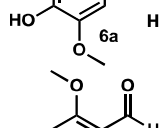
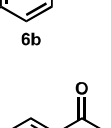
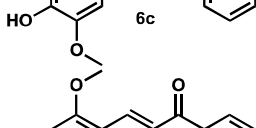
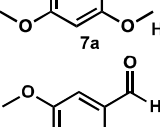
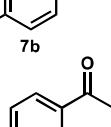
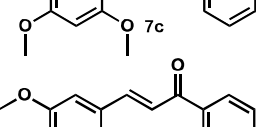
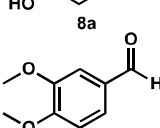
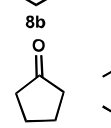
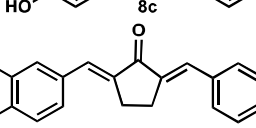
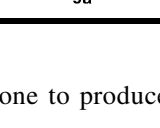
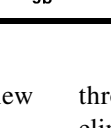
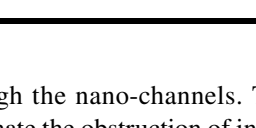
The influence of reaction temperature in the performance of AISBA-15 (41) catalyst for compound 1c synthesis was also investigated in the range of 25 to 110 °C, in toluene for a period of 120 min and the results are shown in Table 2. It was observed that up to 40 °C, there is product formation as the reactant molecules did not acquire sufficient activation energy to cross the barrier for product formation. As the gradual increase of reaction temperature from 60 to 100 °C, the yield of compound 1c also increased from 25 to 84%. No considerable increase in the product yield was observed with further increase in temperature up to 110 °C (Table 2, Entry 1–6). But different amount of the product yield of compound 1c was observed viz., 91% and 86% under azeotropic reaction conditions at the reaction temperature of 100 °C and 110 °C, respectively. The decrease of product yield to 86% is due to the possible self-condensation of vanillin at higher temperatures (> 110 °C) (Table 2, Entry 7, 8). This suggests that the optimum reaction temperature to obtain significantly high product yield was 100 °C under azeotropic conditions.

### 3.2.5 Effect of substituents

The scope and restrictions of utilizing heterogeneous AISBA-15 catalysts in this catalytic system were studied by the introduction of different substituted aryl aldehydes with 1-tetralone and *p*-hydroxyacetophenone to synthesise new chalcone molecules. The results are shown in Table 3. The reaction of 1-tetralone or *p*-hydroxyacetophenone with different substituents on aryl aldehydes did not show much effect on the yields of the product (< 85%) and reaction rate. This clearly indicates that AISBA-15 (41) catalyst was effective over a wide range of aryl aldehyde reactions with



**Table 3** AISBA-15 (41) acid catalyzed Claisen–Schmidt condensation reaction to synthesise new chalcone derivatives

Entry	Aldehydes	Ketones	Product	Isolated yield of product (%)	Product melting point (°C)
1				91	129–131
2				93	155.1–155.5
3				89	112–113
4				85	119–120
5				95	115.1–116.2
6				90	217.1–217.8
7				86	176–178
8				90	82–83
9				92	198.5–199.5

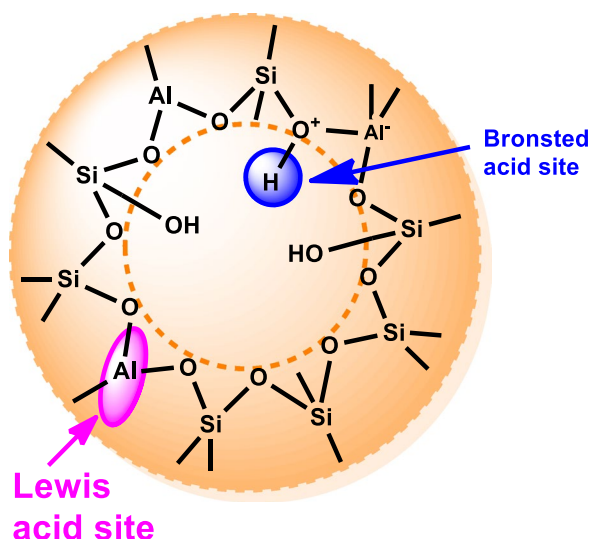
1-tetralone and *p*-hydroxyacetophenone to produce new chalcone derivatives.

Based on the structural, physicochemical and catalytic applications of AISBA-15, the excellent catalytic properties could be ascribed to the following factors. (i) The presence of Brønsted/Lewis active sites (Scheme 3) on AISBA-15 catalysts could have catalysed Claisen–Schmidt condensation reaction more efficiently. (ii) The extraordinary textural properties of AISBA-15 surface could assume the key factor for improved catalytic performance and selectivity towards the synthesis of compound 1c. The uniform distribution of pore channel with larger pores on AISBA-15 samples could enable easy diffusion of reactants and elution of products

through the nano-channels. This could also minimize or eliminate the obstruction of internal mass exchange. Consequently, the access for the active sites on the catalyst by the reactants was made possible by the larger pore size of 54 Å.

### 3.2.6 Reaction mechanism

The mechanism of AISBA-15 catalysed Claisen–Schmidt condensation to synthesise new chalcone is shown in Scheme 4. This reaction occurred between 1-tetralone and vanillin adsorbed on the active sites of catalyst surface. The carbonyl oxygen of vanillin protonated by interaction with the acidic sites of the catalyst produced



**Scheme 3** Schematic wall structure of Al incorporated SBA-15 (AISBA-15) materials

benzylideneoxonium (I). The nucleophilic attack of tautomerised carbon of 1-tetralone on the protonated carbonyl carbon of vanillin yielded 2-(hydroxy(phenyl)methyl)-3,4-dihydronaphthalen-1(2H)-one (II), followed by proton migration and hydration process. Thus, the chalcone was formed promptly.

### 3.2.7 Catalyst reusability tests

The reuse of AISBA-15 (41) catalyst was tested under optimised conditions after recovering the catalyst by filtration. Catalyst regeneration was carried out by washing the catalyst with toluene and then with methanol, finally the catalyst dried at 100 °C. The regenerated catalyst was again used to study the catalyst lifetime and its catalysing ability. The

regenerated catalyst sustained a high performance with 92% of product yield for three runs with no misfortune in its execution. Diminished catalytic activity of 89.5 and 88% in the product yield was observed in fourth and fifth runs, respectively as depicted in Fig. 8.

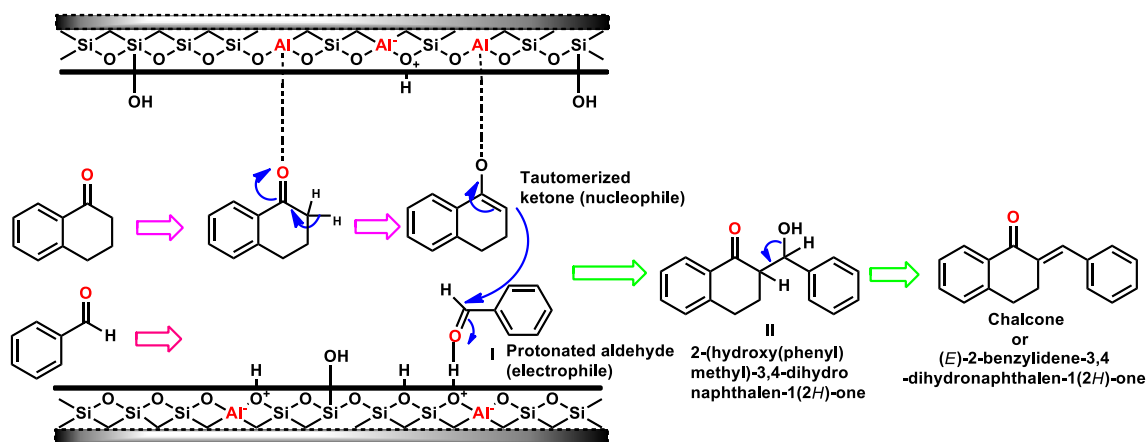
The physical properties of the chalcones synthesised were resolved and molecular structures were affirmed by  $^1\text{H}$  &  $^{13}\text{C}$  NMR and FTIR spectra. From the  $^1\text{H}$  NMR spectral ( $J_{\text{H}\alpha\text{-H}\beta} = 16 \text{ Hz}$ ) information, it can be observed that the synthesised chalcones were geometrically unadulterated. It is also remarkable to note that the ethylene moiety in the enone linkage of chalcones is in *trans*-conformation.

## 3.3 Bio evaluation of novel chalcones

### 3.3.1 Antioxidant studies

Humans are more prone to diseases induced by reactive species including ROS and RNS. Therefore, it becomes essential to search for more efficient antioxidants that can neutralize these reactive species. In the present study we have evaluated the ability of synthesised chalcones to serve as potent antioxidants. Several assays including 1-diphenyl-2-picrylhydrazyl radical (DPPH $\cdot$ ), hydroxyl radical (OH $\cdot$ ) scavenging activity and reducing ability have been evaluated. The antioxidant activity of all the chalcones were evaluated by their scavenging ability and is reported as  $\text{EC}_{50}$  values. TBHQ was used as a positive control and curcumin as a standard drug.

All the synthesised new compounds were screened for DPPH radical scavenging activity using TBHQ as positive control and curcumin as a standard drug. The activity of chalcones was tested at different concentration in the range of 0 to 500  $\mu\text{M}$  and the  $\text{EC}_{50}$  values are presented in Table 4. Out of all the synthesized compounds, compound 2c exhibited significant activity as antioxidant (Table 4).  $\text{EC}_{50}$  value



**Scheme 4** Possible reaction mechanism for the synthesis of chalcone

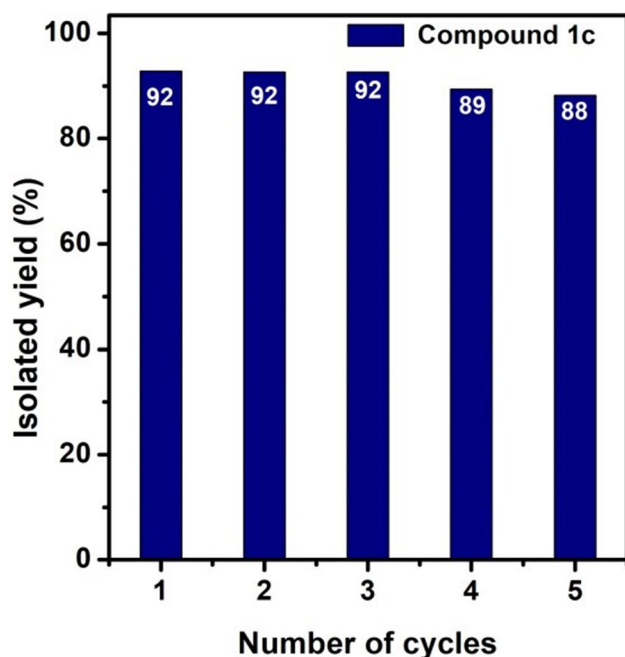


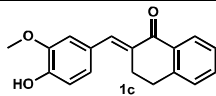
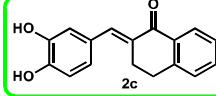
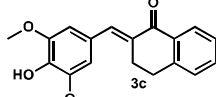
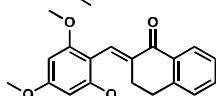
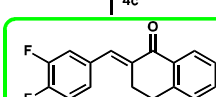
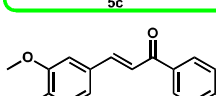
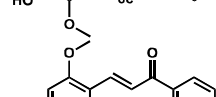
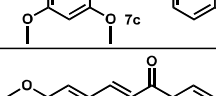
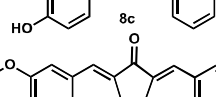
**Fig. 8** Reusability test of AISBA-15 (41) catalyst on the synthesis of compound 1c

for compound 2c was 6.67  $\mu\text{M}$  and that of curcumin is 2.93  $\mu\text{M}$ .

The high antioxidant potential of compound 2c could be attributed to the presence of two active –OH groups at 3 and 4 positions, which effectively induce the formation of an intramolecular hydrogen bond. The increased antioxidant activity could be due to the formation of stable phenoxy radical by abstraction of free H atoms that are not utilized in the bond formation. It was very clear from Fig. S2 that with the increase in concentration, the free radical scavenging activity of chalcones also increased and its percentage scavenging values are provided in Table S1.

Numerous biological processes generate hydrogen peroxide and serve as transmitters for various redox signals. Chalcones have been reported to possess peroxides scavenging activity [10]. The ability of the synthesised novel chalcones to effectively scavenge hydrogen peroxide was tested and the results were compared with curcumin and are depicted in Figure S3. The percentage scavenging ability is given in Table S1 and the  $\text{EC}_{50}$  values are given in Table 4. Among all the tested new chalcones the compound 5c was found to be more effective than other compounds. The  $\text{H}_2\text{O}_2$ -scavenging activity, to a great extent depends on the electron-donating ability of chalcones. Upon substituting the aromatic ring with electron donating groups (F group), the nucleophilicity of the chalcone increases, thereby enhancing its  $\text{H}_2\text{O}_2$ -scavenging ability. This could be due to their increasing tendency to lose electrons easily. Instead if the compounds possess the tendency to lose hydrogen atom, it

**Table 4**  $\text{EC}_{50}$  values of in vitro antioxidant activities of chalcones

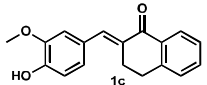
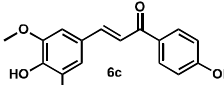
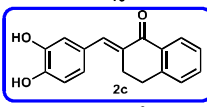
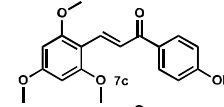
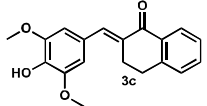
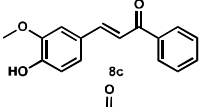
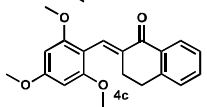
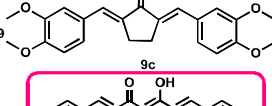
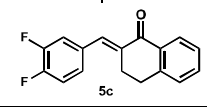
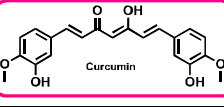
Entry	Samples	DPPH ( $\mu\text{M}$ )	$\text{H}_2\text{O}_2$ ( $\mu\text{M}$ )	FRP ( $\mu\text{M}$ )
1		45,25 $\pm$ 3,02	366,09 $\pm$ 24,41	51,4 $\pm$ 3,42
2		6,67 $\pm$ 0,55	51,23 $\pm$ 3,42	5,71 $\pm$ 0,38
3		18,56 $\pm$ 2,8	123,52 $\pm$ 8,24	26,27 $\pm$ 1,75
4		-	-	-
5		-	26,83 $\pm$ 1,79	4,97 $\pm$ 0,33
6		26,02 $\pm$ 1,74	134,99 $\pm$ 9,0	21,65 $\pm$ 1,44
7		-	113,34 $\pm$ 7,56	-
8		10,97 $\pm$ 0,73	8,35 $\pm$ 0,56	10,20 $\pm$ 0,68
9		-	-	-
10	TBHQ	14,20 $\pm$ 0,95	67,09 $\pm$ 4,47	49,30 $\pm$ 3,29
11 <sup>a</sup>	Curcumin	71,64	29,13	-

<sup>a</sup>The  $\text{EC}_{50}$  values of curcumin are based on the literature (see Ref. [29])

will lead to less  $\text{H}_2\text{O}_2$ -scavenging potential. The  $\text{EC}_{50}$  value was found to be 26.83  $\mu\text{M}$  for compound 5c and 67.09  $\mu\text{M}$  and 27.14  $\mu\text{M}$  for TBHQ and curcumin, respectively.

The reducing ability of all the synthesised new chalcones was tested and the results are shown in Figure S4 and  $\text{EC}_{50}$  values are presented in Table 4. Reducing power of chalcones gradually increased with simultaneous increase in the concentration of chalcone and its percentage efficiencies are provided in Table S1. A strong antioxidant activity could be revealed from the high absorbance values. Among all synthesised chalcones, the compounds 5c, 2c, 6c, and 3c gave highest  $\text{EC}_{50}$  value of about 4.97  $\mu\text{M}$ , 5.71  $\mu\text{M}$ , 21.65  $\mu\text{M}$  and 26.27  $\mu\text{M}$ , respectively. It can be noted that –OH and

**Table 5** Quenching and binding parameters of the HSA-Chalcone systems

Entry	Compound	$K_{SV}$ ( $10^5 M^{-1}$ )	$K_q$ ( $10^{13} M^{-1}$ )	$K_b$ ( $10^5 M^{-1}$ )	$n$	Entry	Compound	$K_{SV}$ ( $10^5 M^{-1}$ )	$K_q$ ( $10^{13} M^{-1}$ )	$K_b$ ( $10^5 M^{-1}$ )	$n$
1		1.31	2.18	0.91	0.94	6		0.63	1.05	1.33	1.06
2		2.15	3.59	2.39	1.00	7		0.82	1.37	1.05	1.03
3		0.66	1.10	0.74	1.04	8		1.26	2.10	1.51	1.00
4		1.74	2.90	0.17	0.82	9		0.24	0.40	0.12	0.93
5		7.82	13.03	0.01	0.49	10 <sup>a</sup>		2.11	3.52	2.62	0.86

<sup>a</sup>The  $K_{SV}$ ,  $K_q$ ,  $K_b$ , and  $n$  values of Curcumin are based on the literature (see Ref [23])

–F groups of chalcones play a significant role to trap and neutralize free radicals, singlet and triplet oxygen, peroxides, etc. The reducing ability of the samples can be monitored by the change in optical density at 700 nm.

### 3.3.2 HSA binding studies

The fluorescence emission spectra of HSA in the presence of varying concentrations of chalcones were evaluated and the results are given in Table 5. HSA has a characteristic emission band maximum at 344 nm. Hypochromism associated with a slight blue shift was observed with the addition of increasing concentrations of chalcones, indicating the interaction between chalcones and HSA. A good linear relationship was observed in the Stern–Volmer plot with different experimental concentrations of the quencher. The slope of Stern–Volmer plot was used to calculate the value of  $K_{SV}$  (Table 5). The bimolecular quenching constant  $K_q$  as calculated using Eq. 2 is estimated to be  $7.00 \times 10^{12} \text{ dm}^3 \text{ mol}^{-1} \text{ s}^{-1}$ . The maximum value of scatter collision quenching constant as reported in the literature for various quenchers with biopolymers, is  $\sim 2.00 \times 10^{10} \text{ dm}^3 \text{ mol}^{-1} \text{ s}^{-1}$ . The larger values of quenching rate constant could be due to static quenching instead of collisional phenomenon. The number of binding sites ( $n = 1$ ) indicate the presence of a single independent binding site on HSA for chalcones. The obtained results revealed that the binding constant of all synthesised chalcones bound with HSA have the following order,  $2c > 8c > 6c > 7c > 1c > 3c > 4c > 9c > 5c$ . Our results demonstrate that the chalcones interact with the protein via the phenolic hydroxyl groups present in the chalcone. It is

interesting to observe that compound 2c, displayed a binding constant of  $2.39 \times 10^5 \text{ M}^{-1}$  which is comparable to that of curcumin,  $2.628 \times 10^5 \text{ M}^{-1}$ .

## 4 Conclusion

New vanillin derived chalcone and its derivatives were successfully synthesised using heterogeneous AISBA-15 mesoporous solid acid catalyst under non-conventional and eco-friendly conditions. AISBA-15 (41) catalyst exhibited excellent catalytic performance with 98% conversion of 1-tetralone and a selectivity of 100% for compound 1c (91% yield) in a time span of 120 min as compared to AISBA-15 (129) and AISBA-15 (210) catalysts. This could be because of more acidic sites on catalyst surface and easy access of reactants into nano-channels of AISBA-15 (41) with large pore size of 54 Å. New chalcone derivatives synthesised herein showed very good antioxidant activity and some were found to be more active than the parent chalcone (compound 8c), and standard antioxidant (curcumin). Further the synthesised chalcones possessed appreciable binding affinity towards albumin (HSA). The binding constant of compound 2c was found to be  $2.390 \times 10^5 \text{ M}^{-1}$  which is comparable to curcumin ( $K_b = 2.628 \times 10^5 \text{ M}^{-1}$ ). The reported chalcones confirmed their suitability for a host of possible biological applications with antioxidant activity and protein binding abilities. It is also believed that the synthesised new chalcones could create a new path towards discovering new drugs with less side effects.

**Acknowledgement** One of the authors (G. Chandrasekar) is grateful to the Deanship of Scientific Research of Imam Abdulrahman Bin Faisal University for the financial support under the project (2019-036-Sci).

## References

- B.M. Choudary, M.L. Kantam, C.R. Reddy, K.K. Rao, F. Figueras, *J. Mol. Catal. A* **146**, 279 (1999)
- P. Anand, A.B. Kunnumakkara, R.A. Newman, B.B. Aggarwal, *Mol. Pharm.* **4**, 807 (2007)
- S. Raghavan, P. Manogaran, B.K. Kuppuswami, G. Venkatraman, K.K. Narasimha, *Med. Chem. Res.* **24**, 4157 (2015)
- M.S. Alam, S.M. Rahman, D.U. Lee, *Chem. Pap.* **69**, 1118 (2015)
- R. Kalirajan, S.U. Sivakumar, S. Jubie, B. Gowramma, B. Suresh, *Int. J. Chemtech. Res.* **1**, 27 (2009)
- A.U. Rahman, Amsterdam: Elsevier publishers (2005).
- M.R. Ahmad, V.G. Sastry, N. Bano, S. Anwar, *Arab. J. Chem.* **9**, S931 (2016)
- T.H. Bui, N.T. Nguyen, P.H. Dang, H.X. Nguyen, M.T. Nguyen, *SpringerPlus* **5**, 1789 (2016)
- M.Z. Gibson, M.A. Nguyen, S.K. Zingales, *J. Med. Chem.* **14**, 333 (2018)
- B.T. Kim, J.C. Chun, K.J. Hwang, *Bull. Korean Chem. Soc.* **29**, 1125 (2008)
- T. Venkatesh, Y.D. Bodke, R. Kenchappa, S. Telkar, *J. Med. Chem.* **6**, 440 (2016)
- T.A. Geissman, R.O. Clinton, *J. Am. Chem. Soc.* **68**, 697 (1946)
- S. Paul, R. Gupta, *Indian J. Chem. Technol.* **5**, 263 (1998)
- A. Russell, S.F. Clark, *J. Am. Chem. Soc.* **61**, 2651 (1939)
- M.E. Zwaagstra, H. Timmerman, M. Tamura, T. Tohma, Y. Wada, K. Onogi, M.Q. Zhang, *J. Med. Chem.* **40**, 1075 (1997)
- D.S. Breslow, C.R. Hauser, *J. Am. Chem. Soc.* **62**, 2385 (1940)
- G. Chandrasekar, M. Hartmann, V. Murugesan, *J. Nanosci. Nanotechnol.* **14**, 4683 (2014)
- G. Chandrasekar, M. Hartmann, M. Palanichamy, V. Murugesan, *Catal. Commun.* **8**, 457 (2007)
- B.J. Melde, B.J. Johnson, P.T. Charles, *Sensors* **8**, 5202 (2008)
- X. An, J. Zhao, F. Cui, G. Qu, *Arab. J. Chem.* **10**, S1781 (2017)
- Y. Fan, Q. Si, Y. Liu, X. Wang, H. Liu, M. Xie, *Anal. Sci.* **33**, 493 (2017)
- S.C. Gupta, S. Prasad, J.H. Kim, S. Patchva, L.J. Webb, I.K. Priyadarsini, B.B. Aggarwal, *Nat. Prod. Rep.* **28**, 1937 (2011)
- B.M. Liu, J. Zhang, A.J. Hao, L. Xu, D. Wang, H. Ji, S.J. Sun, B.Q. Chen, B. Liu, *Spectrochim. Acta A* **155**, 88 (2016)
- A. Murugesan, R.M. Gengan, R. Rajamanikandan, M. Ilanchelian, C.H. Lin, *Syn. Commun.* **47**, 1884 (2017)
- K.M. Naik, S.T. Nandibewoor, *J. Lumin.* **143**, 484 (2013)
- T. Tronina, P. Strugała, J. Popłoński, A. Włoch, S. Sordon, A. Bartmańska, E. Huszcza, *Molecules* **22**, 1230 (2017)
- S.Z.-Jahromi, H.M.-Torshizi, *J. Biomol. Struct. Dyn.* **36**, 1329 (2018).
- T. Ak, İ. Gülçin, *Chem. Biol. Interact.* **174**, 27 (2008)
- S.K. Borra, P. Gurumurthy, J. Mahendra, *J. Med. Plants Res.* **7**, 2680 (2013)
- P. Poprac, K. Jomova, M. Simunkova, V. Kollar, C.J. Rhodes, M. Valko, *Trends Pharmacol Sci.* **38**, 592 (2017)
- E. Bendary, R.R. Francis, H.M. Ali, M.I. Sarwat, S. El Hady, *Ann. Agric. Sci.* **58**, 173 (2013)
- N.M. Hamada, N.Y. Abdo, *Molecules* **20**, 10468 (2015)
- M.G.-Cazalilla, J.M.M.-Robles, A. Gurbani, E.R.-Castellón, A.J.-López, *J. Solid State Chem.* **180**, 1130 (2007).
- P. Elamathi, M.K. Kolli, G. Chandrasekar, *Int. J. Nanosci.* **17**, 1760010 (2018)
- P. Elamathi, G. Chandrasekar, *Catal. Lett.* **148**, 1758 (2018)

**Publisher's Note** Springer Nature remains neutral with regard to jurisdictional claims in published maps and institutional affiliations.